J. Great Lakes Res. 32:63–76
Internat. Assoc. Great Lakes Res., 2006

Classifying and Forecasting Coastal Upwellings in Lake Michigan Using Satellite Derived Temperature Images and Buoy Data

Stefan Plattner[1,†], Doran M. Mason[1,*], George A. Leshkevich[1], David J. Schwab[1], and Edward S. Rutherford[2]

[1]*NOAA Great Lakes Environmental Research Laboratory*
2205 Commonwealth Boulevard
Ann Arbor, Michigan 48105

[2]*University of Michigan School of Natural Resources and Environment*
Institute for Fisheries Research
212 Museum Annex Bldg.
1109 N. University
Ann Arbor, Michigan 48109

ABSTRACT. *Coastal upwellings are common in the Great Lakes but have lacked enumeration and systematic classification of spatial extent, frequency, duration, and magnitude. Near real-time sea surface temperature (SST) images derived from the Advanced Very High Resolution Radiometer (AVHRR) provide indices of upwelling events, but visual inspection of daily images can be tedious. Moreover, the definition of what constitutes an upwelling from AVHRR data is subjective. We developed a semi-automated method to classify upwellings during the period of thermal stratification using daily, cloud-free surface temperature charts from AVHRR SST data. Then we statistically evaluated the location, frequency, magnitude, extent, and duration of upwelling events in Lake Michigan from 1992–2000. Further, we analyzed meteorological data from the National Data Buoy Center buoys in an attempt to improve the reliability of the classification and to provide a means for future forecast of coastal upwelling. Although variable, upwelling events along the western shoreline were preceded by 4 days of southerly and west-to-northwesterly winds, while upwelling events occurring along the eastern shore were preceded by 4 days of northerly winds. Probability of an upwelling event occurring was a function of the direction-weighted wind speed, reaching a 100% probability at direction weighted wind speeds of 11 m s^{-1} for the western shore. Probability of an upwelling occurrence along the east coast reached 73% at 11 m s^{-1} and 100% at 13 m s^{-1}. Continuous measurements of wind data with a sufficient temporal resolution are required during the entire upwelling season to improve the predictability of upwellings.*

INDEX WORDS: *Upwelling, Lake Michigan, AVHRR, Great Lakes.*

INTRODUCTION

Coastal upwelling, a phenomenon found in large stratified lakes, estuaries, and oceans, occurs when the continued forcing of offshore winds moves warm epilimnetic water away from the coast, transporting cold water from the hypolimnion to the surface. In the Laurentian Great Lakes, this exchange of water masses results in the short-term nutrient enrichment of surface waters (Haffner *et al.* 1984, Dunstall *et al.* 1990) and the redistribution or change in the nearshore plankton communities (Heufelder *et al.* 1982, Haffner *et al.* 1984, Dunstall *et al.* 1990, Megard *et al.* 1997). Moreover, upwellings may be responsible for reduction in species richness in benthic communities (Barton 1986, Kilgour *et al.* 2000), higher biomass and production of some benthic invertebrates (Nalepa *et al.* 2000), and changes in fish distributions through behavioral thermal regulation or passive advection (Heufelder *et al.* 1982, Fitzsimons *et al.* 2002). Upwellings may also cause mortality in adult fish due

*Corresponding author. E-mail: Doran.Mason@noaa.gov
Current address: NOAA Atlantic Oceanographic Meteorological Laboratory, 4301 Rickenbacker Causeway, Miami, FL 33149.
†Current address: German Aerospace Center DLR, German Remote Sensing Data Center DFD, D-82234 Oberpfaffenhofen, Germany.

to rapid decrease in water temperatures (Heufelder *et al.* 1982).

Significance of upwelling is clear, however, to quantify this physical forcing on ecological processes, one is faced with how to classify and quantify upwelling events on a lake-wide basis. For example, Mortimer (1971) used temperature data from municipal water intakes around the lake and bathythermograph casts from trans-lake car ferries. But, due to the high variation of water temperatures in the nearshore zone, and the lack of sufficient spatial coverage, these data are not adequate for resolving the spatial distribution of lake temperatures (Schwab *et al.* 1999). Moreover, Bolgrien and Brooks (1992) visually identified upwelling events occurring in Lake Michigan using Advanced Very High Resolution Radiometer (AVHRR) data of sea surface temperature (SST); however, their main focus was identifying and tracking the development of thermal bars. Thus, the question remains- how to classify and quantify upwelling events across space and time while trying to minimize biases associated with subjective classification, and to eliminate the tedium of visually inspecting the SST maps.

In this study, we developed a semi-automated classification algorithm to identify, classify, and quantify (location, frequency, magnitude, extent, and duration) upwelling events in Lake Michigan when the lake is thermally stratified using AVHRR SST data. We then used this information to evaluate the history of upwelling in Lake Michigan from 1992–2000. Lastly, we used wind data from the National Data Buoy Center (NDBC) buoys and upwelling data to forecast when an upwelling may occur.

METHODS

We used Great Lakes Surface Environmental Analysis (GLSEA) composite surface temperature charts produced by the CoastWatch program at the National Oceanic and Atmospheric Administration's Great Lakes Environmental Research Laboratory (NOAA/GLERL) (Leshkevich *et al.* 1992, Schwab *et al.* 1999) to develop our semi-automated upwelling classification algorithm and to assess the history of upwelling events in Lake Michigan. The GLSEA charts are daily composites of temperature images produced from the thermal AVHRR channels of NOAA's polar orbiting weather satellites (see example in Fig. 1). Data are geo-corrected, cloud-masked, and edge-enhanced before the daily composite chart is computed. Temperature values of cloud-covered areas are derived from the previous-day composite image. For longer periods of cloud cover, a 5-day average is used to estimate surface water temperature in the cloud covered region. As the GLSEA composite charts are daily, geometrically corrected, cloud-free surface temperature fields, the GLSEA composite charts are a better tool for this study than the original satellite imagery, which may lack one or more of these qualities. A detailed description of the methodology can be found in Schwab *et al.* (1999). GLSEA temperature composite charts are available for the Great Lakes beginning in 1992 at a spatial resolution of 2.6 km^2. We confined our study to Lake Michigan for the years 1992–2000 and only for the period of time in which Lake Michigan was thermally stratified.

Identification of an Upwelling Event

To detect upwelling events during the 9-year period (1992–2000) from the available 3,069 daily GLSEA charts, a histogram of the surface temperature by day was created for each year and plotted as a time series-contour graph (see example in Fig. 2). We identified upwelling events by evaluating the daily histogram on the time-series contour plot. Given that an upwelling event causes a substantial drop in the minimum temperature, an upwelling may be identified by a broadening of the daily histogram, which may also be characterized by a skewed distribution at the low temperatures in SST histogram (Fig. 3). In the time series histogram, these significant decreases in temperature can be identified by dips in the minimum temperature (Fig. 2).

Significant deviations from the overall mean surface temperature may occur for reasons other than from upwelling events, particularly during spring when the lake warms from south to north. To prevent these situations from being interpreted as an upwelling in our analysis, Lake Michigan was divided into three regions- North (N), Central (C), and South (S), prior to creating the time series histograms (Fig. 4b). Then, for each regional time series histogram, a temperature threshold (t) was established,

$$t_{i,j} = T_{median,i,j} - 4°C,$$

where T_{median} is the median temperature for region i on day j. Pixels with temperatures at or below the threshold were classified as upwelling areas. This

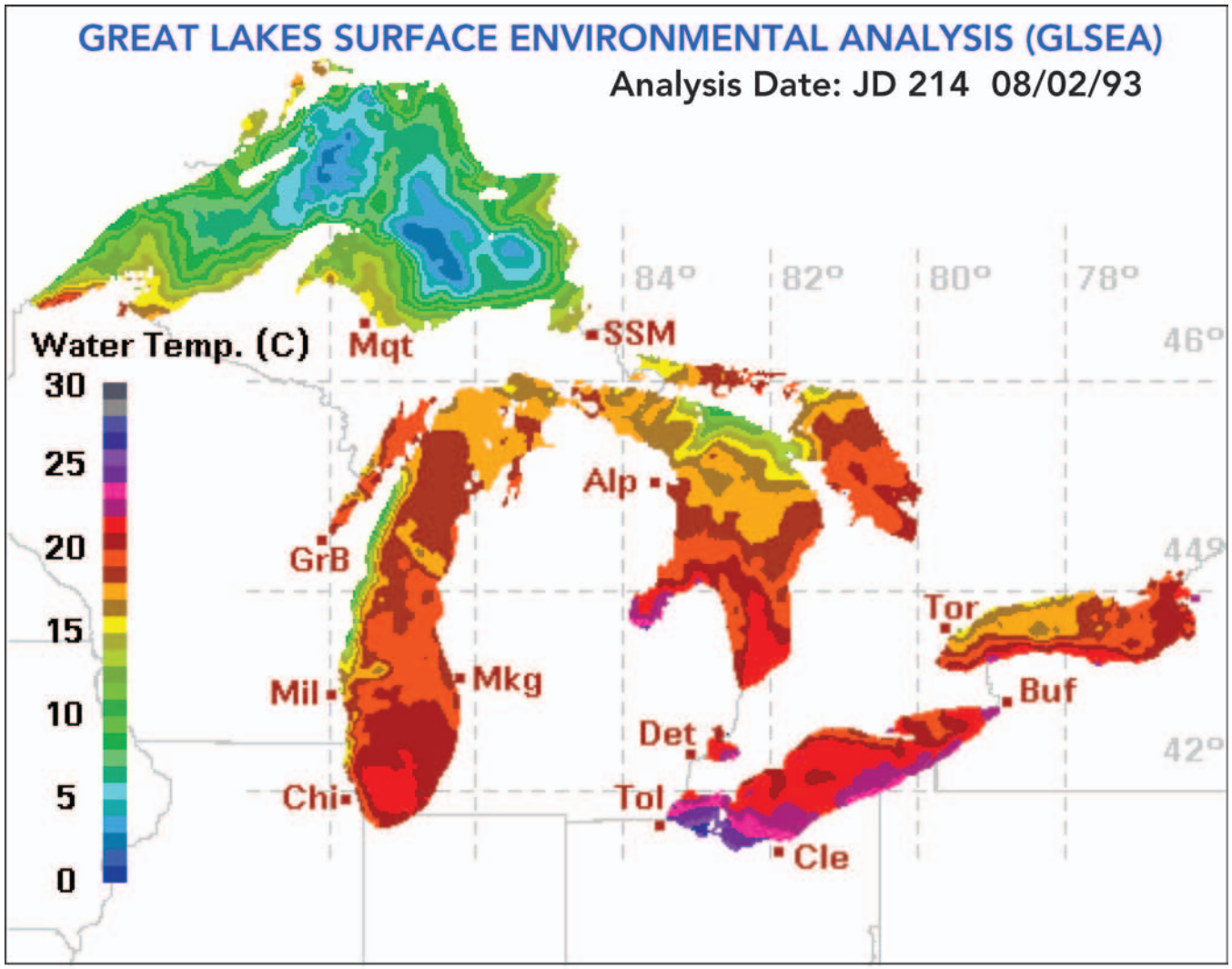

FIG. 1. GLSEA SST map of 2 August 1993, showing upwelling events along the western shore of Lake Michigan, and northern Lake Huron. GLSEA SST charts are produced by the Great Lakes CoastWatch Program at the NOAA, Great Lakes Environmental Research Laboratory.

index was chosen because it makes upwelling sufficiently distinguishable from most other local variations of the water surface temperature. The median value of SST was preferred rather than the mean, since the median is less sensitive to changes in temperature at the tail of the distribution, where an upwelling will be detected (Fig. 3). Four degrees C was selected as the constant as a result of empirical testing; it was found that a difference of 4°C provided a reasonable temperature threshold for upwelling classification. We tested other definitions and threshold values, but by careful analysis of several different types of upwelling events, we found this algorithm to be the most robust. The definition was then applied to the time series histogram; an upwelling event was identified where the threshold intersected the yearly contour plot of temperature histograms (Fig. 2). Note, however, that our method classified upwelling events where there was a surface thermal gradient, i.e., during the stratified season. The beginning and the end of the upwelling season (detectable by our method) is marked by the date when median sea surface temperature rises above or falls below a value less than 4°C above the temperature of the hypolimnion.

After the classification, a visual examination of the pre-classified situations was made in order to eliminate unclear situations, errors due to cloud

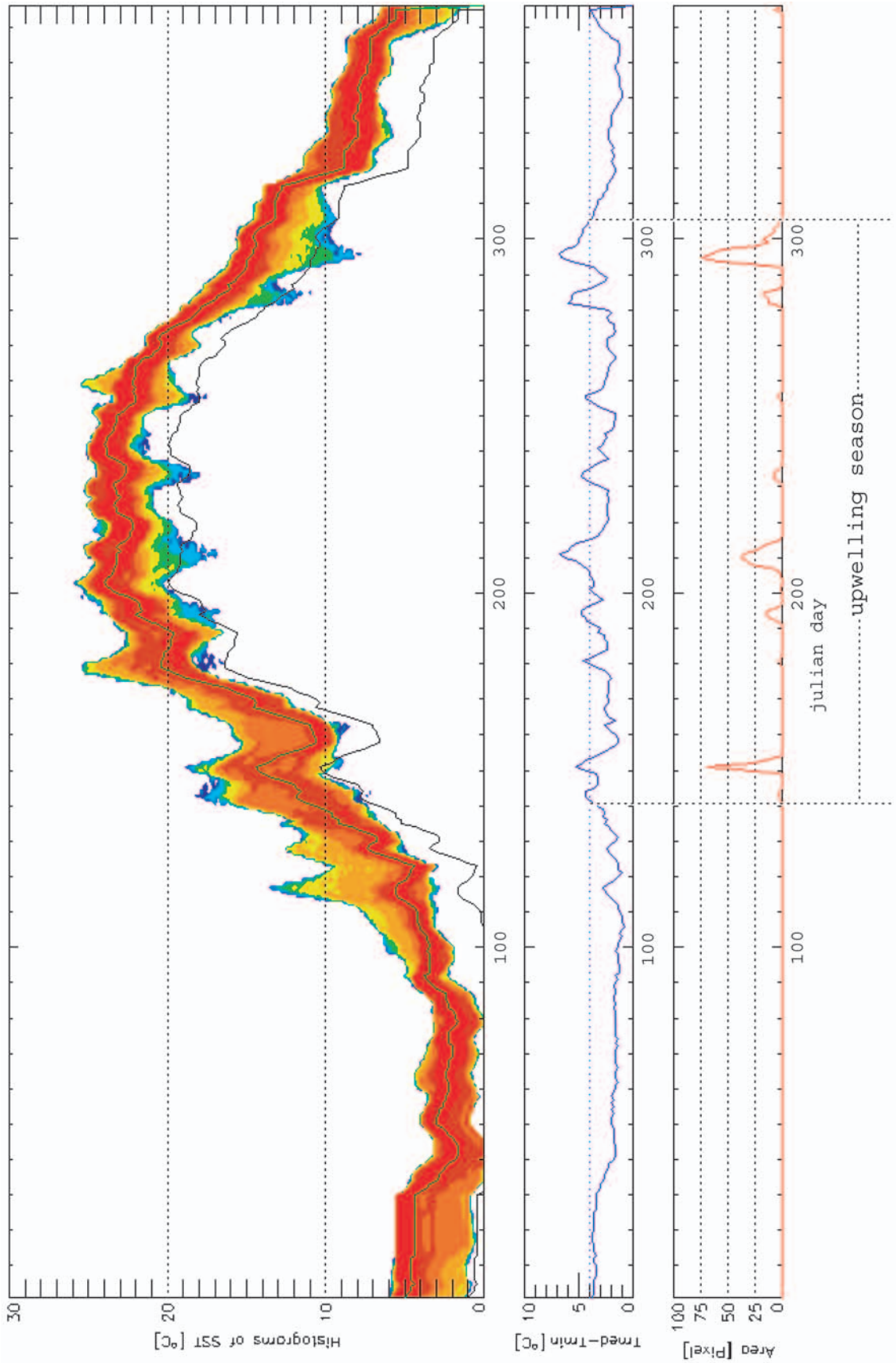

FIG. 2. *Top: Contour plot of daily sea surface temperature (SST) histograms, southern Lake Michigan, 1998. The green line is the median of SST and the black line represents the classification threshold (T_{median}–4°C). Middle: Plot of T_{median}–T_{min}: the dotted horizontal line is the classification threshold (4°C). Values exceeding the classification threshold delineate an upwelling event. Bottom: Number of pixels in the GLSEA chart where threshold is exceeded (upwelling area).*

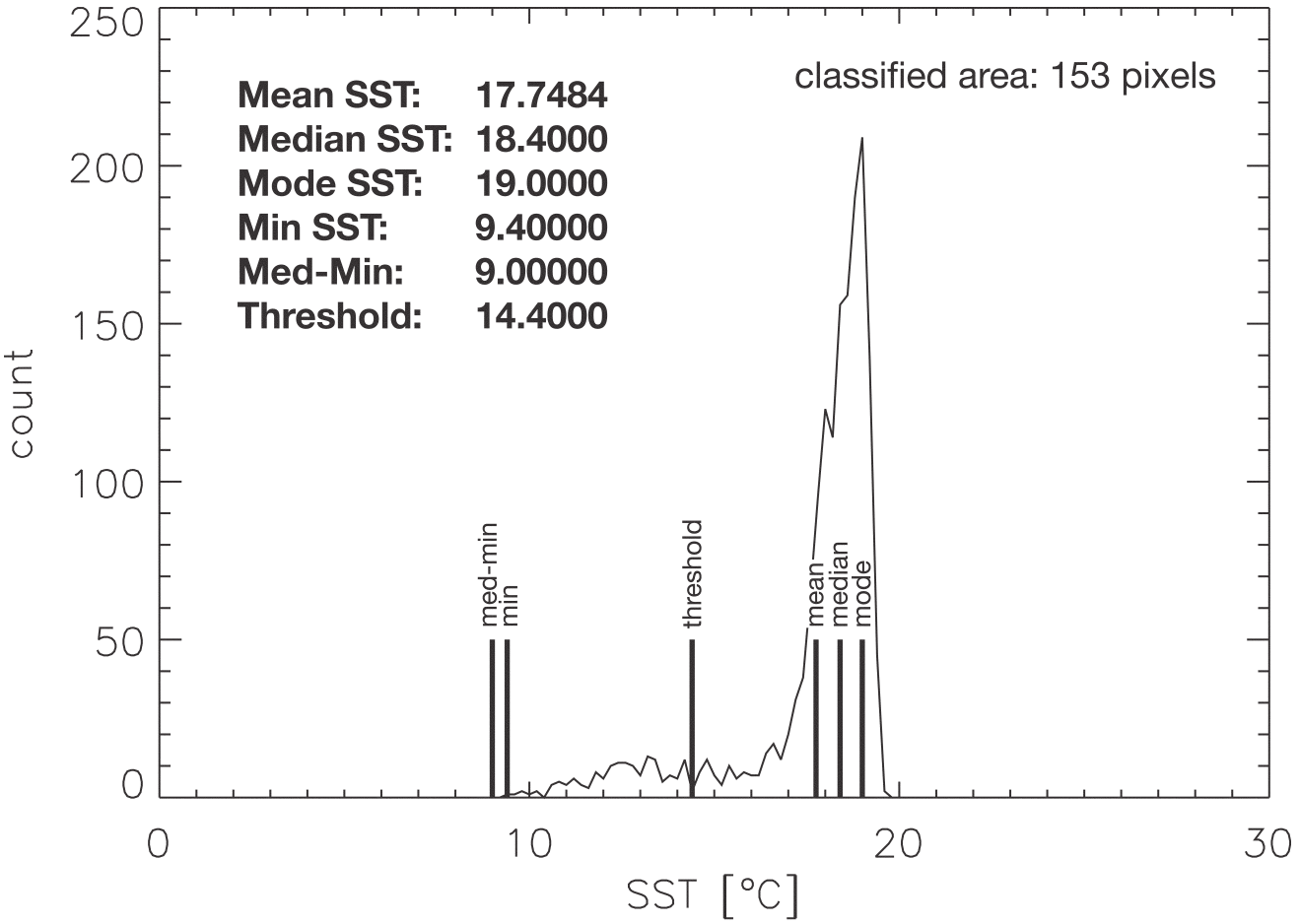

FIG. 3. Histogram of GLSEA SST map, central Lake Michigan, of 2 August 1993. The shape of this histogram is typical of upwelling events during the stratified period of the lake. The upwelling leads to a significant drop of the minimum temperature as well as to a broadening of the histogram.

masking problems, and erroneously classified areas which occurred in some rare cases. Figure 4c–d is an example of the three regions in Lake Michigan and a classified upwelling area.

Upwelling Statistics

Using our classification scheme, we determined the location, frequency, duration, extent, and magnitude of upwelling events in any given year. Frequency is simply the number of upwelling events occurring in each of the regions per year. Duration of the upwelling event is the number of days the upwelling event was detectable. Extent is the maximum area occupied by the upwelling. Magnitude is defined as the difference between the median water surface temperature of the region and the minimum water surface temperature within the upwelling area. Since a threshold of $T_{median} - 4°C$ was used to classify the areas of upwelling events, the magnitude of an event had to be at least 4°C in order to be detected.

Relationship between Wind Properties and Upwelling

We used wind data with our classified upwelling events to identify meteorological conditions that would likely create an upwelling event. Wind data (hourly speed and direction) were available from NDBC buoys 45007 (southern Lake Michigan, 42.67N, 87.02W) and 45002 (northern Lake Michigan, 45.31N, 86.42W). These buoys have provided hourly meteorological data since 1979 and 1981, respectively. We selected these two buoys because they are located in the middle of the southern and

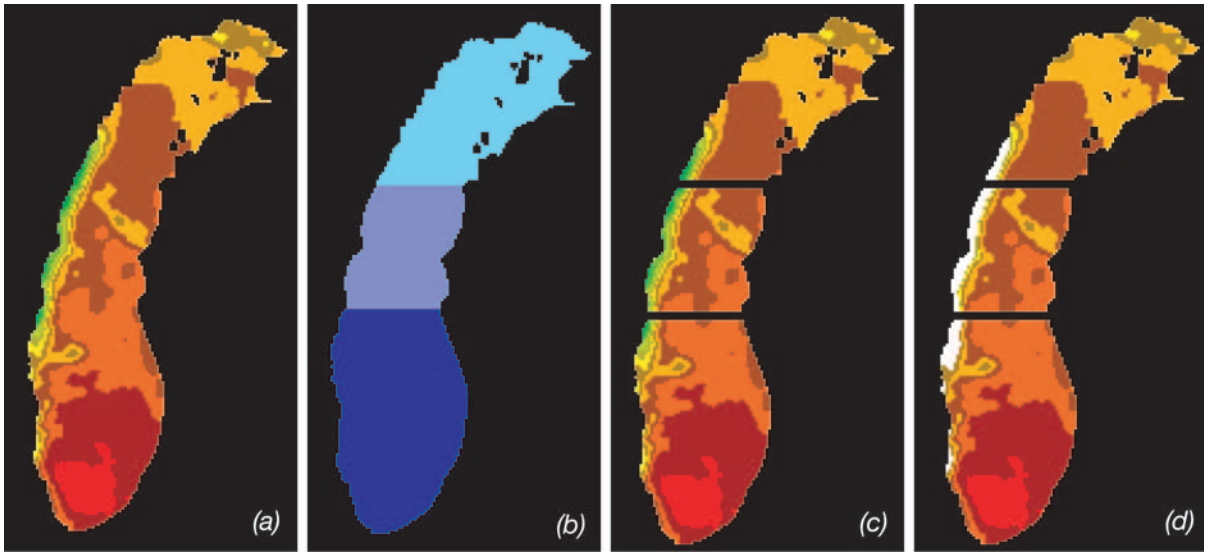

FIG. 4. a) SST of Lake Michigan on 2 August 1993. b) Mask for southern, central and northern Lake Michigan. c) Mask applied to SST map. d) Upwelling areas (white), classified for each section independently.

northern regions, and because other meteorological stations (airports or Coast Guard stations) were found to provide less representative data, and at irregular intervals, which made them unsuitable for a long-term comparison between 1992 and 2000. These wind data were then classified into two categories:

Class A: 5 days prior to an upwelling event, with the fifth day consisting of the first day of the classified upwelling.

Class B: All other days during the detectable upwelling season that showed no upwelling event, and days not within the 5-day window prior to an upwelling.

To determine the probability that an upwelling event will occur, we first weighted wind velocity by direction for both categories of wind. Differential direction polar histograms (polar plots) of each region were normalized by their maximum:

$$\text{dirfactor}(\text{dir}) = \frac{f(\text{dir})}{f_{max}}$$

where f(dir) is the frequency of each wind direction (1-degree steps), and f_{max} is the highest frequency of a wind direction. The probability that an upwelling event would occur based on the wind data was then determined by

$$P = \frac{n_p}{n_{total}}$$

where n_p is the number of hours at a certain direction-weighted wind speed during all pre-upwelling periods (class A), and n_{total} is the total number of hours at the same direction-weighted wind speed during all non-upwelling periods of the season, including all pre-upwelling periods (class A + class B).

RESULTS

Upwelling Season

The first detectable upwelling event of the thermally stratified season generally occurred between the end of June and the end of July, but was as late as the beginning of August (Table 1). The detectable upwelling season usually ended during November; but in some cases, upwelling events could be observed in early December. The average duration of the upwelling season (i.e., duration of the thermal stratification) was about 132 days (~4.5 months), but ranged from 109 days (~3.5 months) to 171 days (~5.5 months) (Table 1).

Frequency and Location

Frequency of upwelling events ranged from two to eight per year and averaged about five per year

TABLE 1. Upwelling season, i.e., period when the lake is completely stratified [beginning and ending dates (month/day), duration (days)], total number of days of upwelling by region, and percent of the upwelling season with upwelling events in Lake Michigan from 1992–2000.

Year	Begin	End	Days	South	Central	North	East	West	Lake Wide	% of season w/ upwelling
1992	6/21	11/12	144	75	67	38	24	78	102	70.8%
1993	7/10	11/6	119	64	39	36	10	54	64	53.8%
1994	7/22	11/23	124	86	77	37	14	95	109	87.9%
1995	7/11	11/6	118	73	36	24	5	74	79	66.9%
1996	8/2	12/5	125	70	73	43	22	59	81	64.8%
1997	7/24	11/10	109	54	51	34	26	46	72	66.1%
1998	6/24	11/15	144	35	50	26	11	47	58	40.3%
1999	6/18	12/6	171	70	54	18	34	55	89	52.0%
2000	6/28	11/5	130	14	31	9	19	21	40	30.8%
Mean	7/7	11/15	131.6	60.1	53.1	29.4	18.3	58.8	77.1	58.6%

TABLE 2. Number of upwelling events by region in Lake Michigan from 1992–2000, and percent of upwellings occurring in each region for all years.

Year	South	Central	North	East	West	Lake Wide
1992	2	2	1	1	1	2
1993	4	3	3	1	3	4
1994	5	4	2	2	5	7
1995	3	4	2	1	3	4
1996	4	4	2	1	3	4
1997	3	2	1	2	1	3
1998	5	6	1	3	4	7
1999	7	5	2	5	3	8
2000	2	4	1	3	2	5
Mean	3.9	3.8	1.7	2.1	2.8	4.9
Total	35	34	15	19	25	44
Percent	80.0%	77.6%	34.1%	43.2%	56.8%	

for the 9-year period (Table 2). Regionally, upwelling events occurred in each of our predefined regions (southern, central, and northern) and on the western and the eastern shorelines of the lake. Greatest percentage (57%) of upwelling events occurred on the western shoreline of Lake Michigan, with 92% of all of these events partly or entirely within the central region. In contrast, 89% of all east coast upwelling were found partly or entirely in the southern region. For the northern region, only one upwelling event was classified on the eastern shoreline for the entire 9-year period. Regions most likely to show an upwelling were Milwaukee to Door Peninsula on the western shore, and Muskegon to Frankfort on the eastern shore. Regardless of the coast (west or east), the southern part of Lake Michigan showed the highest percentage of upwelling events with 80% of all upwellings affecting this region, followed by the central (78%) and then northern areas (34%) (Table 2).

Duration

Total number of upwelling days ranged from 40 to 102 and averaged about 77 days per year (Table 3), representing 31%–71% (mean = 59%) of the upwelling season (Table 1). The western shoreline tended to have a greater number of days per year, averaging about 59 days (range: 21–95 days), compared to the eastern shoreline, which averaged about 18 days per year (range: 5–34 days). Duration of a single upwelling event also varied among years and regions, averaging about 16 days per event (range: 2–78 days) (Table 3). Upwelling events oc-

TABLE 3. Mean duration of upwelling events (minimum, maximum) by region for Lake Michigan from 1992–2000 where duration is number of days an upwelling event is observed.

Year	South	Central	North	East	West	Lake Wide
1992	37.5 (15,60)	33.5 (20,47)	38.0 (38,38)	24.0 (24,24)	78.0 (78,78)	51.0 (24,78)
1993	16.0 (13,24)	13.0 (9,16)	12.0 (7,18)	10.0 (10,10)	18.0 (13,24)	16.0 (10,24)
1994	17.2 (3,33)	19.3 (5,33)	18.5 (4,33)	7.0 (3,11)	19.0 (4,46)	15.6 (3,46)
1995	24.3 (8,42)	9.0 (2,21)	12.0 (8,16)	5.0 (5,5)	24.7 (9,42)	19.8 (5,42)
1996	17.5 (7,36)	18.3 (6,42)	21.5 (19,24)	22.0 (22,22)	19.7 (7,44)	20.3 (7,44)
1997	18.0 (9,32)	25.5 (16,35)	34.0 (34,34)	13.0 (9,17)	46.0 (6,46)	24.0 (9,46)
1998	7.0 (2,13)	8.3 (2,26)	26.0 (26,26)	3.7 (2,5)	11.8 (3,27)	8.3 (2,27)
1999	10.0 (2,23)	10.8 (3,17)	9.0 (5,13)	6.8 (2,13)	18.3 (13,23)	11.1 (2,23)
2000	7.0 (7,7)	7.8 (5,15)	9.0 (9,9)	6.3 (5,7)	10.5 (6,15)	8.0 (5,15)
1992-2000	15.5 (2, 60)	14.1 (2, 47)	17.7 (4, 38)	8.7 (2, 24)	21.2 (3, 78)	15.8 (2,78)

curred for a greater duration on the western shoreline, averaging about 21 days per event (range: 3–78 days), compared to the eastern shoreline which averaged about 9 days per event (range: 2–24 days). Duration of a single event was similar across the south, central, and northern zones (mean range 14–18 days).

Extent

The extent (maximum area) of the classified upwelling events varied among regions and years (Table 4). The range of maximum annual extent along the western coast (33–5,095 km^2) was similar to that of the eastern shore (27–5,671 km^2), but the greatest mean extent was almost three times higher

TABLE 4. Mean extent (km^2) of an upwelling event (minimum, maximum) by region for Lake Michigan from 1992–2000 where extent is measured at the greatest area (km^2) of an upwelling event. Italic numbers: percent of region area (south, central, north) or entire lake area (east, west, lake wide).

Year	South	Central	North	East	West	Lake Wide
1992	2,156 (432, 3,880) *9.4 (1.9, 16.9)*	1,119 (243, 1,994) *10.0 (2.2, 17.9)*	879 (879, 879) *5.5 (5.5, 5.5)*	432 (432, 432) *0.9 (0.9, 0.9)*	5,041 (5,041, 5,041) *10.0 (10.0, 10.0)*	2,737 (432, 5,041) *5.4 (0.9, 10.0)*
1993	779 (169, 1,561) *3.4 (0.7, 6.8)*	1,061 (865, 1,270) *9.5 (7.7, 11.4)*	603 (590, 1,176) *3.7 (1.8, 7.3)*	169 (169, 169) *0.3 (0.3, 0.3)*	2,598 (1,749, 3,905) *5.2 (3.5, 7.8)*	1,991 (169, 3,905) *4.0 (0.3, 7.8)*
1994	677 (27, 1,426) *2.9 (0.1, 6.2)*	1,004 (60, 3,069) *9.0 (0.5, 27.5)*	1,190 (74, 2,305) *7.4 (0.5, 14.3)*	615 (27, 1,203) *1.2 (0.1, 2.4)*	1,366 (60, 5,095) *2.7 (0.1, 10.1)*	1,151 (27, 5,095) *2.3 (0.1, 10.1)*
1995	714 (216, 1,419) *3.1 (0.9, 6.2)*	473 (47, 919) *4.2 (0.4, 8.2)*	213 (81, 344) *1.3 (0.5, 2.1)*	94 (94, 94) *0.2 (0.2, 0.2)*	1,317 (587, 1,926) *2.6 (1.2, 3.8)*	1,011 (94, 1,926) *2.0 (0.2, 3.8)*
1996	760 (243, 1,973) *3.3 (1.1, 8.6)*	669 (54, 1,602) *6.0 (0.5, 14.3)*	1,129 (54, 2,203) *7.0 (0.3, 13.7)*	5,671 (5,671, 5,671) *11.3 (11.3, 11.3)*	698 (316, 1,433) *1.4 (0.6, 2.9)*	1,941 (316, 5,671) *3.9 (0.6, 11.3)*
1997	784 (128, 1,946) *3.4 (0.6, 8.5)*	1,385 (479, 22,910) *12.4 (4.3, 20.5)*	358 (358, 358) *2.2 (2.2, 2.2)*	388 (277, 499) *0.8 (0.6, 1.0)*	4,535 (4,535, 4,535) *9.0 (9.0, 9.0)*	1,770 (277, 4,535) *3.5 (0.6, 9.0)*
1998	188 (27, 500) *0.8 (0.1 ,2.2)*	305 (33, 878) *2.7 (0.3, 7.9)*	763 (763, 763) *4.7 (4.7, 4.7)*	101 (67, 134) *0.2 (0.1, 0.3)*	781 (33, 1,904) *1.6 (0.1, 3.8)*	490 (33, 1,904) *1.0 (0.1, 3.8)*
1999	295 (47, 648) *1.3 (0.2, 2.8)*	332 (54, 743) *3.0 (0.5, 6.7)*	429 (94, 763) *2.7 (0.6, 4.7)*	402 (47, 1,034) *0.8 (0.1, 2.1)*	715 (175, 1,323) *1.4 (0.3, 2.6)*	520 (47, 1,323) *1.0 (0.1, 2.6)*
2000	135 (101, 169) *0.6 (0.4, 0.7)*	201 (40, 547) *1.8 (0.4, 4.9)*	175 (175, 175) *1.1 (1.1, 1.1)*	110 (40, 189) *0.2 (0.1, 0.4)*	439 (169, 709) *0.9 (0.3, 1.4)*	242 (40, 709) *0.5 (0.1, 1.4)*
1992-2000	618 (27, 3,880) *2.7 (0.1, 16.9)*	619 (3, 3,069) *5.5 (0.3, 27.5)*	660 (54, 2,305) *4.1 (0.3, 14.3)*	580 (27, 5,671) *1.2 (0.1, 11.3)*	1,456 (33, 5,095) *2.9 (0.1, 10.1)*	1,078 (27, 5671) *2.1 (0.1, 11.3)*

TABLE 5. Mean magnitude (°C) of upwelling events (maximum) by region for Lake Michigan 1992–2000. Only maximum magnitude is shown in the parenthesis as the minimum is always 4°C, see text for details.

Year	South	Central	North	East	West	Lake Wide
1992	8.3 (11.4)	6.2 (7.8)	8.4 (8.4)	5.2 (5.2)	11.4 (11.4)	8.3 (11.4)
1993	8.0 (9.6)	7.9 (9.0)	7.9 (9.2)	6.0 (6.0)	9.3 (9.6)	8.5 (9.6)
1994	6.7 (9.6)	6.7 (9.0)	6.3 (7.8)	5.9 (7.4)	6.3 (9.6)	6.2 (9.6)
1995	7.8 (8.4)	5.5 (7.2)	5.1 (5.8)	5.2 (5.2)	7.8 (8.4)	7.2 (8.4)
1996	7.9 (12.4)	6.0 (7.2)	6.1 (8.0)	12.4 (12.4)	6.5 (7.6)	8.0 (12.4)
1997	6.8 (9.0)	6.1 (7.2)	6.8 (6.8)	5.7 (6.4)	9.0 (9.0)	6.8 (9.0)
1998	5.5 (6.8)	5.3 (7.2)	5.6 (5.6)	4.7 (4.8)	5.7 (7.2)	5.3 (7.2)
1999	6.3 (8.0)	5.6 (6.8)	6.1 (7.2)	5.9 (7.2)	6.9 (8.0)	6.3 (8.0)
2000	5.8 (6.2)	5.7 (6.4)	5.8 (5.8)	5.6 (6.2)	6.2 (6.4)	5.8 (6.4)
1992–2000	6.9 (12.4)	6.0 (9,0)	6.5 (9.2)	5.9 (12.4)	7.1 (11.4)	6.6 (12.4)

along the western coast (1,456 km^2) compared to the eastern coast (580 km^2). Mean maximum extent of upwelling events for the 9-year period was similar in the southern (618 km^2) and central (619 km^2) basins, with the extent of upwelling in the northern basin being slightly greater (660 km^2). The mean extent of all upwelling events in Lake Michigan from 1992 to 2000 was 1,078 km^2.

Magnitude

Magnitude (maximum difference of temperature to the median) of upwelling events varied from a minimum of 4°C (by definition) to a maximum of 12.4°C, with the greatest mean magnitude (7.1°C) occurring along the western shoreline, and the highest peak magnitude (12.4°C) occurring along the eastern shoreline (Table 5). Maximum mean magnitude of upwelling events was greatest in the southern basin relative to the central and northern basin. The mean magnitude of all upwelling events in Lake Michigan for the whole period was 6.6°C.

Wind Conditions

For the western shore, upwelling events were preceded by 4 days of southerly and west-to-northwesterly winds (Fig. 5), while upwelling events occurring along the eastern shore were preceded by four days of northerly winds (Fig. 6). The probability of an upwelling event occurring was a function of the direction-weighted wind speed (Fig. 7). The southern buoy (45007) shows better results, reaching a 100% upwelling probability at direction weighted wind speeds of 11 m s^{-1} for the western shore. Probability for the east coast reaches 73% at 11 m s^{-1} and 100% at 13 m s^{-1}.

DISCUSSION

Thermal satellite imagery products of the CoastWatch program offer the opportunity for a synoptic view of the lake surface at a high resolution on a daily basis. In contrast to thermal *in situ* data, it represents the only means to measure the extent of short-term, local features of water surface temperature (e.g., upwelling events) in the Great Lakes. However, there are limitations. A spatial resolution of 2.6 km^2 is sufficient to detect medium to large sized upwelling events, but smaller events, occurring as a narrow strip of cold water close to the shore, will likely be missed.

Temporal resolution is another limitation. In principle, the daily resolution of the GLSEA charts is sufficient for detecting upwelling events with duration of at least 1 day. However, in the compositing process, which combines satellite image data for 5 days in order to smooth transitions from cloudy to clear conditions (Schwab *et al.* 1999), the temporal resolution can deteriorate. During long periods of cloud cover over the lake, temporal resolution decreases, so that even events with duration of several days can be missed. However, this is more likely to occur in the spring and fall, outside the upwelling season. For example, at the end of the year 2000, two of these situations, with duration of more than 20 days, occurred. There, according to the GLSEA charts, water surface temperature maintained a level of 11–14°C until the beginning of December, erroneously prolonging the season of potentially detectable upwelling. The supposed end of the season was empirically corrected to Julian day 310 (5 November).

The upwelling season was limited and variable among years. The beginning of this period is determined by the progression rate of the thermal bar,

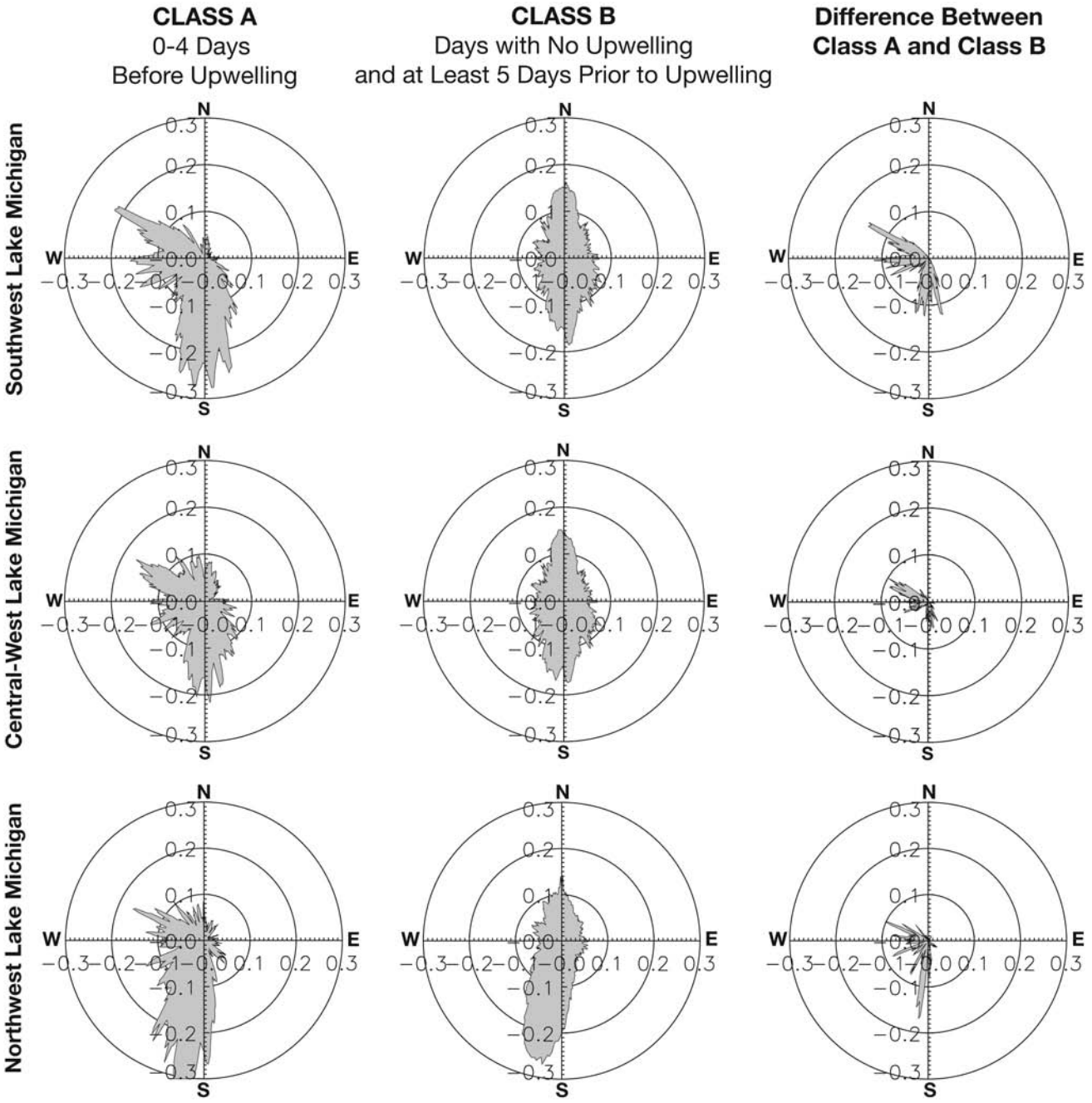

FIG. 5. Polar diagrams of wind directions during upwelling seasons for years 1992–2000. Class A, 0–4 days before upwelling; Class B, days with no upwelling and at least 5 days prior to an upwelling. Unit: directional hours per day (h_d/d). For class definitions see text.

when the lake warms from the coast toward the center during spring. Steep temperature gradients and smaller areas of remaining cold water in the center of the lake would lead to a false classification if the temperature index alone is used and no visual examination of the automatically classified areas is made. However, a certain state of stratification, with an already developed thermocline and warmer surface temperatures, is needed to meet the requirements for the emergence of upwelling. Typically, the upwelling season ends in November, which is the typical time for the fall turnover. Dur-

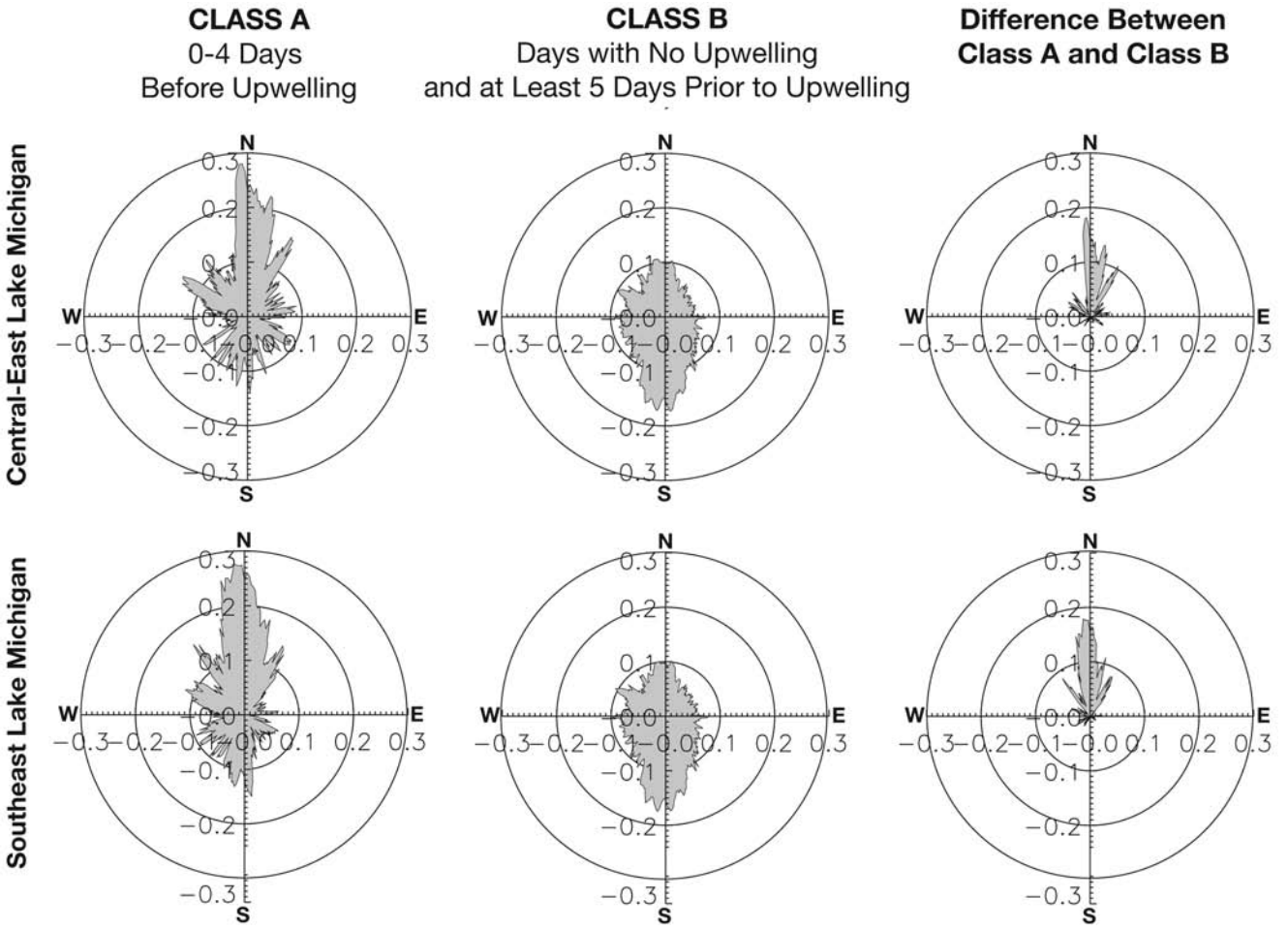

FIG. 6. Polar diagrams of wind directions during upwelling seasons for years 1992–2000. Class A, 0–4 days before upwelling; Class B, days with no upwelling and at least 5 days prior to an upwelling. Unit: directional hours per day (h_d/d). For class definitions see text

ing many years, fall turnover is driven by an extended upwelling at the western shore of Lake Michigan. As a result, the decline of the surface temperature progresses from west to east in these years. The end of the upwelling season is defined when the median temperature difference between surface waters and hypolimnetic waters falls below 4°C.

The majority of coastal upwellings in Lake Michigan during the study period occurred on the western coast. The average duration and mean extent of upwellings were almost three times higher on the west coast than the east coast. The difference in average durations between the western and eastern coast would have been even higher if not for a single extended upwelling event that occurred in 1996 on the northeastern shore, where this phenomenon seems to be unusual.

Care must be exercised when interpreting the upwelling statistics. For example, there was an apparent long duration upwelling event of 78 days in 1992. Note that the 78-day upwelling event did not occur at the same position for the entire 78 days. Rather, it first developed in the northern part of the lake (Door Peninsula) and slowly migrated southward. The process then spread from west to east and was classified as an upelling given that the warmer surface water at the eastern part of the lake kept the median temperature of the entire lake sufficiently high. A clear delineation of the initial upwelling and the breakdown of the stratification is not possible. This leads to the classification of this very long upwelling event (see 1992 GLSEA

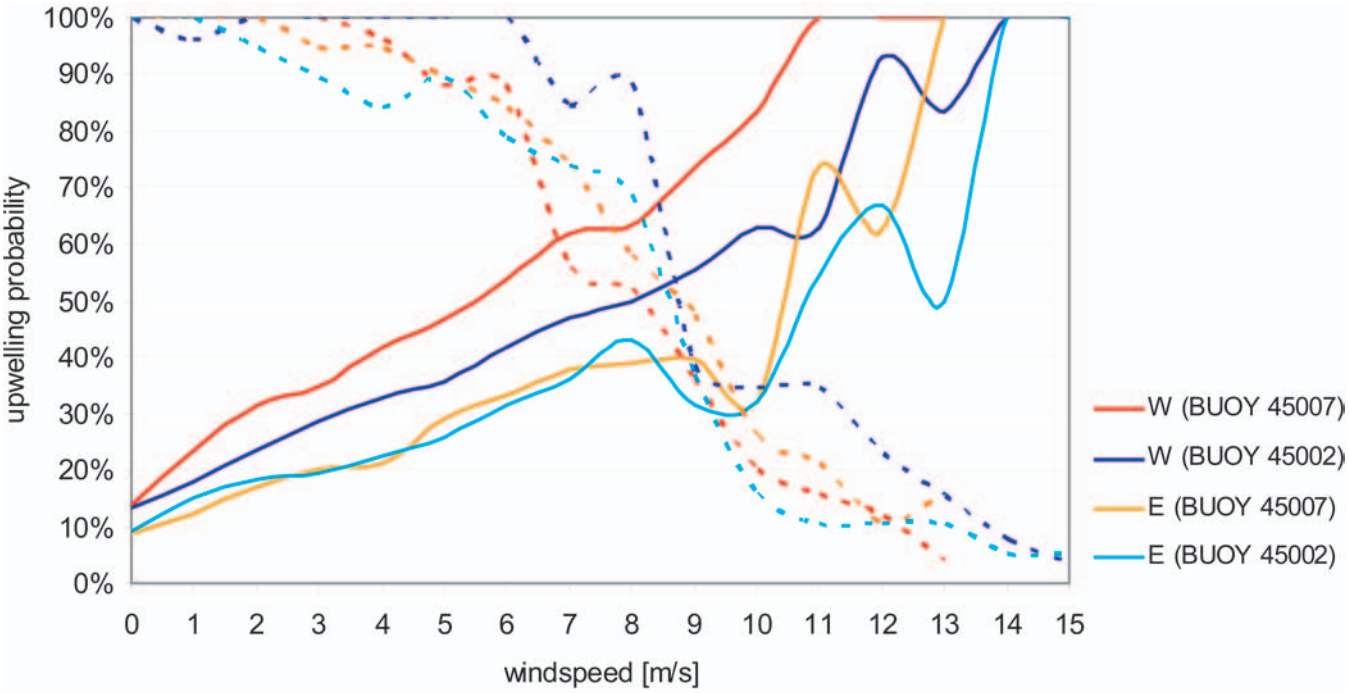

FIG. 7. Probability of coastal upwelling event occurring as a function of direction-weighted wind speed (solid lines), for western and eastern coast of Lake Michigan. Dotted lines show the cumulative distribution of percentage of upwelling events that are preceded by winds of that speed. Data from Buoys 45007 and 45002 are compared.

animation, http://coastwatch.glerl.noaa.gov/glsea/glsea.html).

Another uncommon event was observed in August 1994 at the northernmost tip of Lake Michigan. This upwelling extended from the mouth of Green Bay along the shoreline of Michigan's Upper Peninsula and continued at the northern coast of Lake Huron, where it reached its maximum extent. The upwelling was likely caused by continuous winds from the west and northwest directions. Predominant winds in that area during August were westerly with several north westerly events during the month. In spite of the fact that upwellings at the eastern and western coast are caused by winds from opposite directions, upwellings in the GLSEA imagery may appear on the same day at both the eastern and western shores. This is the case if wind direction changes by 180° degrees and a new upwelling occurs at the opposite coast before the preceding upwelling has entirely disappeared.

The magnitude of upwelling events observed in the southern basin tended to be greater than in the northern basin because the lake surface in southern Lake Michigan is typically warmer than in the north, while the temperature of the hypolimnium is more balanced over the extent of the lake. For the same reason, upwellings during periods with higher surface temperatures (late July, August, early September) had higher magnitudes than those in early summer and fall. Finally, the longer upwelling events tended to show higher magnitudes, although the larger areas of cold water in these situations led to a lower median surface temperature and thus, to a potentially lower magnitude, as it is defined as $T_{median}–T_{min}$. Therefore a positive correlation between duration, extent, and magnitude usually exists.

Years with a lower upwelling frequency generally tended to show higher mean durations of single events. During the period from 1992 to 2000, 1992 was the year with the lowest frequency but with the highest average duration. Attempts to use wind data from NDBC buoys 45007 and 45002 to forecast upwellings or to infer possible missed upwellings in the GLSEA classification for the years 1992 to 2000 turned out to be very difficult. Although high wind speeds of more than 10 m s^{-1} may increase the upwelling probability to values near 100%, this result has to be regarded critically and carefully. Statistically, these high probabilities are based on 10 or

fewer wind events at that speed during the 9-year period. As a result, the probabilities in Figure 7 start to swing heavily at their upper end, as the number of available samples decreases.

Reliable forecast of upwellings using wind data was impeded by the high variability in wind velocity, direction, and duration. Situations with relatively stable wind speeds from constant directions were found in pre-upwelling periods, but were rare. Instead, highly variable velocities combined with unsteady directions were found in these periods as well. An attempt to lower the adverse effect of this high variability on the predictability of upwelling events was made by averaging wind speeds over different time intervals from 6 to 72 hours, but did not lead to better results. For averaging, mean, median, and maximum values of velocity were used alternatively. In addition, the distribution of variance of wind directions in pre-upwelling and non-upwelling periods was examined, showing no sufficient correlation with pre-upwelling situations to improve the predictability.

Our inability to determine the exact time of an upwelling from daily GLSEA charts may have affected our ability to forecast upwelling from wind data. Since upwellings and their causal meteorological conditions may operate over the time scale of hours, and the GLSEA charts depict conditions of the lake surface integrated over 24 hours, our attempts to condense these charts with wind data to forecast upwellings may have been adversely affected. However, defining the pre-upwelling class (class A) as a 5-day period prior to the GLSEA-derived starting days (4 days prior to and the first day when the upwelling can be seen in the GLSEA charts) turned out to give the highest correlation. Presumably, a more accurate determination of the start time of each event might make upwellings more predictable. Using the near real-time AVHRR satellite imagery, available four to six times daily, could help determine a more accurate start time for each event if the coastal areas of interest are cloud free.

Since wind conditions are highly variable both in speed and direction, it is still unclear how duration of winds with a certain speed and direction affect upwellings. High wind speeds of more than 10 m s^{-1}, prevailing for a few hours can cause upwellings, as can winds of a lower velocity but longer duration—as long as they continue to blow from directions likely to cause coastal upwelling. Reasonable explanations of the cause of an upwelling are possible in many cases by interpreting the time series of wind speed and direction. But in most situations, the high variability in wind speed, direction, and duration makes it difficult to use a statistical approach to determine which wind conditions reliably cause upwellings. As mentioned earlier, our attempts to use averaged wind speeds to decrease the influence of variability did not increase the predictability of upwelling. However, the results confirm the dependence of upwelling events on higher wind speeds (Fig. 7) and certain wind directions (Figs. 6 and 7), which correspond with those mentioned by Mortimer (1971). Upwellings on the western shore seem not only to be caused by southerly winds, but also by winds from westerly to northwesterly directions. In eastern Lake Michigan, the relation between northerly winds and upwellings is very distinct.

Due to the derived results, it is assumed that a sufficient temporal resolution and accuracy of input data are indispensable for improving the predictability of upwelling events, since the high variability in wind speed and direction makes it difficult to predict upwellings using a statistical approach. To more accurately determine the start of the GLSEA-derived upwellings, it would be useful to use near real-time AVHRR data, routinely available from two NOAA weather satellites (four orbits) or *in situ* measurements of water temperatures. Hourly data, or at least four measurements per day, are recommended to achieve the necessary accuracy.

The use of wind data from meteorological stations located on the shore of Lake Michigan may raise the predictability of upwellings on a more local scale. Using wind data from NDBC buoys 45007 and 45002 led to a more accurate prediction of upwellings on the entire western or eastern shore of Lake Michigan, but performed worse in zonal (north, central, and south) correlations. Since wind speed and direction at the coast may show high deviations from those measured by the buoys, but are supposed to be responsible for local upwelling events at the adjacent section of the shore, this could improve predictability on a more local scale. Again, continuous measurements of wind with sufficient spatial and temporal resolution are needed during the entire upwelling season. Satellite scatterometer derived winds (measured twice daily) (Nghiem *et al.* 2004) and modeled winds could provide the wind data to help improve the forecast of upwelling events by improving the accuracy and frequency of over water wind data.

The ultimate predictive tool for forecasting thermal structure in the lake is a three dimensional nu-

merical hydrodynamic model, such as the Princeton Ocean Model which is used in the Great Lakes Coastal Forecasting System (Schwab and Bedford 1999). In this type of model, numerical weather forecasts are used to drive a lake circulation model to predict currents and three dimensional temperature structures up to three days in advance. This type of system is still in development, but holds considerable promise for operational forecasting of upwelling events.

ACKNOWLEDGMENTS

We thank two anonymous reviewers for helpful comments and suggestions on the manuscript. This work was funded by the National Oceanic and Atmospheric Administration (NOAA) Great Lakes Environmental Research Laboratory (GLERL) and the Cooperative Institute for Limnology and Ecosystems Research (CILER) at the University of Michigan as part of the Summer Student Fellowship Program. Daily GLSEA composite temperature charts as well as the near real-time AVHRR satellite images of the Great Lakes are available on the CoastWatch Great Lakes web site at http://coastwatch.glerl.noaa.gov. This is contribution number 1374 of the NOAA Great Lakes Environmental Research Laboratory.

REFERENCES

Barton, D.R. 1986. Nearshore benthic invertebrates of the Ontario waters of Lake Ontario. *J. Great Lakes Res.* 12:270–280.

Bolgrien, D.W., and Brooks, A.S. 1992. Analysis of thermal features of Lake Michigan from AVHRR satellite images. *J. Great Lakes Res.* 18:259–266.

Dunstall, T.G., Carter, J.C.H., Monroe, G.T., Weiler, R.R., and Hopkins, G.J. 1990. Influence of upwellings, storms, and generation station operation on water chemistry and plankton in the Nanticoke region of Long Point Bay, Lake Erie. *Can. J. Fish. Aquat. Sci*. 47:1434–1445.

Fitzsimons, J.D., Perkins, D.L., and Kruger, C.C. 2002. Sculpins and crayfish in lake trout spawning areas in Lake Ontario: estimates of abundance and egg predation on lake trout eggs. *J. Great Lakes. Res*. 28:421–436.

Haffner, G.D., Yallop, M.L., Hebert, D.N., and Griffiths, M. 1984. Ecological significance of upwelling events in Lake Ontario. *J. Great Lakes. Res*. 10:28–37.

Heufelder, G.R., Jude, D.J., and Tesar, F.J. 1982. Effects of upwelling on local abundance and distribution of larval alewife (*Alosa pseudoharengus*) in eastern Lake Michigan. *Can. J. Fish. Aquat. Sci*. 39:1531–1537.

Kilgour, B.W., Baily, R.C., and Howell, E.T. 2000. Factors influencing changes in the nearshore benthic community on the Canadian side of Lake Ontario. *J. Great Lakes. Res*. 26:272–286.

Leshkevich, G.A., Schwab, D.J., and Muhr, G.C. 1992. Satellite environmental monitoring of the Great Lakes: A review of NOAA's Great Lakes CoastWatch program. *Photogrammetric Eng. and Remote Sensing* 59:371–379.

Megard, R.O., Kuns, M.M., Whiteside, M.C., and Downing, J.A. 1997. Spatial distributions of zooplankton during a coastal upwelling in western Lake Superior. *Limnol. Oceanogr*. 42:827–840.

Mortimer, C.H. 1971. *Large-scale oscillatory motions and seasonal temperature changes in Lake Michigan and Lake Ontario, Parts I and II.* Special report No. 12, University of Wisconsin-Milwaukee, Center for Great Lakes Studies.

Nalepa, T.F., Hartson, D.J., Buchanan, J., Caveletto, J.F., Lang, G.A., and Lozano, S.J. 2000. Spatial variation in density, mean size and physiological condition of the holarctic amphipod Diporeia spp. in Lake Michigan. *Freshwater Biol*. 43:107–119.

Nghiem, S.V., Leshkevich, G.A., and Stiles, B.W. 2004. Wind fields over the Great Lakes measured by the SeaWinds scatterometer on the QuikSCAT satellite. *J. Great Lakes Res.* 30(1):148–165.

Schwab, D.J., and Bedford, K.W. 1999. The Great Lakes Forecasting System. In *Coastal Ocean Prediction,* Coastal and Estuarine Studies 56, eds. C.N.K. Mooers, pp. 157–173. American Geophysical Union, Washington DC.

Schwab, D.J., Leshkevich, G.A., and Muhr, G.C. 1999. Automated mapping of surface water temperature in the Great Lakes. *J. Great Lakes Res.* 25:468–481.

Submitted: 22 August 2004
Accepted: 11 November 2005
Editorial handling: Joseph V. DePinto